PTEP

Prog. Theor. Exp. Phys. **2024** 053B04 (18 pages)
DOI: 10.1093/ptep/ptae060

Importance of Strange Sea to the Charge Radii and Quadrupole Moment of $J^P = \frac{1}{2}^+, \frac{3}{2}^+$ Baryons

Preeti Bhall* and A. Upadhyay

Department of Physics and Material Science, Thapar Institute of Engineering and Technology, Patiala, Punjab, 147004, India

*Email: preetibhall@gmail.com

Received January 17, 2024; Revised April 9, 2024; Accepted April 16, 2024; Published April 17, 2024

A statistical framework in conjugation with the principle of detailed balance is employed to examine the low-energy properties, i.e. charge radii and quadrupole moment, of $J^P = \frac{1}{2}^+$ octet and $J^P = \frac{3}{2}^+$ decuplet baryons. The statistical model relies on the assumption that the baryons can be expanded in terms of quark–gluon Fock states. We systematically apply operator formalism along with the statistical approach to study the charge radii and quadrupole moment of baryons. Based on the probabilities of all possible Fock states in spin, flavor, and color space, the importance of sea with quarks and gluons is studied. The individual contribution of the constituent quarks and sea (scalar, vector, and tensor sea) is explored. Due to the large mass difference between strange and nonstrange content, the SU(3) breaking effect is also investigated. The extent to which strange $q\bar{q}$ pairs are considered in sea is constrained by the mass of hadrons and the free energy of gluons, in accordance with experimental evidence. We focus on the individual contribution of strange and nonstrange sea (g, $\langle u\bar{u}\rangle$, $\langle d\bar{d}\rangle$, and $\langle s\bar{s}\rangle$) accommodability in the respective hadrons for their charge radii and quadrupole moment. The present work has been compared with various theoretical approaches and some known experimental observations. The obtained results may give valuable information for upcoming experimental findings.

Subject Index B69

1. Introduction

Recently, a remarkable discovery in the field of particle physics was celebrated by three Nobel Prizes. Scientists P. Agostini, F. Krausz, and A. L'Huillier were honored with the Nobel Prize in October 2023 for the development of experimental methods that "produce ultra-short pulses of light (measured in attoseconds) to study the electron dynamics in matter." Each advancement motivates physicists to understand better the internal structure of ordinary matter. The low-energy properties (masses, spin distribution, magnetic moment, semileptonic decays, charge radii, etc.) are preferred for study as they reveal the distribution of quarks inside the hadrons. The electromagnetic form factors are basic quantities that provide essential information about the static properties of hadrons. Over the past few years, significant progress has been witnessed in both experimental and theoretical domains in the study of the intrinsic structure of hadrons. In 2022, the new AMBER experiment at the CERN Super Proton Synchrotron (SPS) [1] examined the charge radii of the proton and mesons, the mesonic Parton momentum distributions, and various aspects of hadron spectroscopy. In 2021, the BESIII experiments successfully conducted the first-ever measurement of form factors within the time-like region

Funded by SCOAP[3].

for various baryons [2]. We know that the hadrons, in addition to the constituent quarks, also carry dynamic "sea," which is filled with different flavors of quark–antiquark pairs ($u\bar{u}$, $d\bar{d}$, $s\bar{s}$) and gluons. The importance of the sea is evident from the fact that 30% of the total nucleonic spin is carried by $q\bar{q}$ pairs present in the sea. In 2019, the STAR experiment observed the major contribution of sea antiquarks to the spin distribution of the proton [3]. Also, the strange quark is one of the important components of sea, contributing markedly to the nuclei spin's distribution within quarks and gluons [4,5]. The NuTeV collaboration [6] at Fermilab confirmed the presence of strange quarks. They predicted a nonzero quark contribution to the spin of the nucleon via the strange and nonstrange quark content ratio. The ratio $\frac{2(s+\bar{s})}{u+\bar{u}+d+\bar{d}} = 0.477 \pm 0.063 \pm 0.053$ signifies how much "strangeness" contributes to overall nucleon momentum as compared to other flavors of quarks [7]. Several experiments conducted at MIT-Bates [8], JLab [9–11], and MAMI [12] measured the weak and electromagnetic form factors which characterize the role of strange quarks in the current, charge, and spin structure of the nucleon. Complete information about strange quark effects in the hadronic sea is still being explored. In the pursuit of understanding the strange quark sector thoroughly, several experimental facilities like at FAIR, $\bar{P}$ANDA-GSI [13,14], and the BESIII [15] with J-PARC [16] are intended to perform experiments at the low-energy regime.

The electromagnetic properties of baryons, i.e. charge radii and quadrupole moment, yield important information about internal structure within the nonperturbative regime of quantum chromodynamics (QCD). They describe the spatial charge distribution inside the baryons and provide information about their geometrical size and shape. Experimental predictions of the charge radii of octet particles, i.e. proton ($r_p = 0.8409 \pm 0.0004$ fm), neutron ($r_n^2 = -0.115 \pm 0.0017$ fm^2), and sigma ($r_{\Sigma^-} = 0.78 \pm 0.10$ fm), have been reported by the Particle Data Group (PDG) [17]. For $J^P = \frac{3}{2}^+$ particles, the experimental data are very limited due to their shorter lifetime. In the literature, various theoretical approaches such as the nonrelativistic quark model [18], relativistic quark model [19], light-front holographic method [20], QCD sum rule [21,22], 1/N$_c$ expansion method [23,24], lattice QCD [25,26], chiral constituent quark model (χCQM) [27,28], and General Parameterization (GP) method [29,30] have studied several properties of octet and decuplet baryons. In Ref. [20], the authors computed the form factors, masses, magnetic moment, and charge radii of baryons. Using the QCD sum rule approach in Refs. [21,22], the authors estimated the multipole moments of Δ-baryons. A.J. Buchmann and E.M. Henley [29,30] employed the GP method to calculate the quadrupole moment of nucleons and decuplet baryons. Based on the framework of χCQM, N. Sharma and H. Dahiya [27,28] studied the effect of SU(3) symmetry and its breaking in relation to the different static properties of baryons. In Refs. [25,26], the charge radii of $J^P = \frac{3}{2}^+$ particles have been analyzed in lattice QCD. Despite the significant success in experimental and theoretical areas, the information on the structure of baryons is still not well understood.

For the purpose of better understanding, we study the charge radii and quadrupole moment of $J^P = \frac{1}{2}^+$ octet and $J^P = \frac{3}{2}^+$ decuplet baryons using a statistical model along with the detailed balance principle. In this model, hadrons are considered as an ensemble of quark–gluon Fock states. The principle of detailed balance is associated with the probability of finding different Fock states within the hadrons. The probabilities associated with various Fock states are affected by considering the strange quark in the sea. Our main focus is to examine the individual contributions of strange as well as nonstrange components inside octet and decuplet baryons for the aforementioned properties. To investigate SU(3) symmetry breaking in valence and sea,

we needed to introduce a parameter that studied the effect of strangeness on the charge radii and quadrupole moment. The statistical model successfully examined various static properties such as masses [31], spin distribution [32], and magnetic moments [33,34]. The statistical approach provides a strong base for understanding the quark–gluon dynamics.

The present work is organized as follows: Sect. 2 includes a detailed discussion of the wavefunction of octet and decuplet baryons with sea components. In Sect. 3, the operator formalism is briefly discussed. Section 4 provides details of the statistical method and detailed balance principle, including various quark–gluon Fock states with strange $q\bar{q}$ pairs. Section 5 presents the numerical outcomes of the charge radii and quadrupole moment with SU(3) symmetry and breaking, leading to the conclusion of the present study in Sect. 6.

2. Theoretical formalism

Hadrons are, in the first approximation, composed of constituent quarks like baryons (qqq) and mesons ($q\bar{q}$), with appropriate spin–flavor and color singlet combinations. In QCD, the presence of quark–gluon interaction suggests that a hadron can be understood as having valence quarks, enveloped by a surrounding "sea" that consists of an infinite number of virtual quark–antiquark ($q\bar{q}$) pairs multiconnected through gluons. However, various studies have demonstrated that the sea contribution may change the internal configuration of hadrons and modify their low-energy properties. The "sea" is characterized by its quantum numbers such as flavor, spin, and color. The quantum numbers are chosen in a way that ensures the combined effects of sea and valence quarks yield the intended quantum numbers for the observed baryon. The valence quark wavefunction of the baryon [35] is represented as:

$$\Psi = \Phi(|\phi\rangle|\chi\rangle|\psi\rangle|\xi\rangle) \tag{1}$$

where $|\phi\rangle$, $|\chi\rangle$, $|\psi\rangle$, and $|\xi\rangle$ represent the flavor, spin, color, and space q^3 wavefunctions, respectively. The valence quarks are assumed to be in an S-wave state, ensuring the spatial wavefunction $|\xi\rangle$ is symmetric under the permutation of any two quarks. The color wavefunction $|\psi\rangle$ is entirely antisymmetric, resulting in a color singlet state of the baryon. Consequently, the flavor–spin wavefunction ($|\phi\rangle$, $|\chi\rangle$) is totally symmetric to ensure the overall antisymmetrization of the baryonic wavefunction. On the other side, sea is considered to be flavorless but has appropriate spin and color wavefunctions. For example, if we consider two gluons present in sea, each having spin-1 and color octet "8," the spin and color space will yield the following possibilities:

$$\textbf{Spin} : gg : 1 \bigotimes 1 = 0_s \bigoplus 1_a \bigoplus 2_s,$$
$$\textbf{Color} : gg : 8 \bigotimes 8 = 1_s \bigoplus 8_s \bigoplus 8_a \bigoplus 10_a \bigoplus \bar{10}_a \bigoplus 27_s$$

Here, the subscript "s" and "a" represent the symmetric and antisymmetric combinations of the states, respectively. The total wavefunction consists of three valence quarks with sea components and can be written systematically as follows.

For octet baryons [35]:

$$\begin{aligned}\left|\Phi_{1/2}^{(\uparrow)}\right\rangle = \frac{1}{N}\Big[&\Phi_1{}^{(\frac{1}{2}\uparrow)} H_0 G_1 + a_8\Big(\Phi_8{}^{(\frac{1}{2})} \otimes H_0\Big)^{\uparrow} G_8 + a_{10}\Phi_{10}{}^{(\frac{1}{2}\uparrow)} H_0 G_{\bar{10}} \\ &+ b_1\Big(\Phi_1{}^{(\frac{1}{2})} \otimes H_1\Big)^{\uparrow} G_1 + b_8\Big(\Phi_8{}^{(\frac{1}{2})} \otimes H_1\Big)^{\uparrow} G_8 + b_{10}\Big(\Phi_{10}{}^{(\frac{1}{2})} \otimes H_1\Big)^{\uparrow} G_{\bar{10}} \\ &+ c_8\Big(\Phi_8{}^{(\frac{3}{2})} \otimes H_1\Big)^{\uparrow} G_8 + d_8\Big(\Phi_8{}^{(\frac{3}{2})} \otimes H_2\Big)^{\uparrow} G_8\Big]\end{aligned} \tag{2}$$

where $N^2 = 1 + a_8^2 + a_{10}^2 + b_1^2 + b_8^2 + b_{10}^2 + c_8^2 + d_8^2$.

For decuplet baryons [33]:

$$\left|\Phi_{3/2}^{(\uparrow)}\right\rangle = \frac{1}{N}\Big[a_0\Phi_1{}^{(\frac{3}{2}\uparrow)}H_0G_1 + b_1\Big(\Phi_1{}^{(\frac{3}{2})}\otimes H_1\Big)^{\uparrow}G_1 + b_8\Big(\Phi_8{}^{(\frac{1}{2})}\otimes H_1\Big)^{\uparrow}G_8 + d_1\Big(\Phi_1{}^{(\frac{3}{2})}\otimes H_2\Big)^{\uparrow}G_1 + d_8\Big(\Phi_8{}^{(\frac{1}{2})}\otimes H_2\Big)^{\uparrow}G_8\Big] \tag{3}$$

where $N^2 = a_0^2 + b_1^2 + b_8^2 + d_1^2 + d_8^2$.

Here, N represents the normalization constant. The wavefunction consists of various combinations of both valence and the sea part such as $\Phi_1{}^{(\frac{1}{2}\uparrow)}H_0G_1$, $(\Phi_8{}^{(\frac{1}{2})}\otimes H_0)^{\uparrow}G_8$, $\Phi_{10}{}^{(\frac{1}{2}\uparrow)}H_0G_{\bar{10}}$, etc. For example, the first term of the octet wavefunction $\Phi_1^{(\frac{1}{2})}$ contains the valence spin-$\frac{1}{2}$, flavor octet, and color singlet state along with a sea component having spin-0 (H_0) and a singlet color (G_1) state:

$$\Phi_1^{(\frac{1}{2})}H_0G_1 = \Phi\left(8, \frac{1}{2}, 1_c\right)H_0G_1 \tag{4}$$

The term $b_1(\Phi_1^{(\frac{1}{2})}\otimes H_1)^{\uparrow}G_1$ comes from vector sea (spin-1) combined with the spin-$\frac{1}{2}$ of the core baryon and is written as:

$$b_1\left(\Phi_1^{(\frac{1}{2})}\otimes H_1\right)^{\uparrow}G_1 = \sqrt{\frac{2}{3}}B\left(8, \frac{1}{2}\downarrow\right)H_{1,1} - \sqrt{\frac{1}{3}}B\left(8, \frac{1}{2}\uparrow\right)H_{1,0} \tag{5}$$

In a similar manner, each term in the wavefunction such as $b_1(\Phi_1^{(\frac{3}{2})}\otimes H_1)^{\uparrow}$, $b_1(\Phi_1^{(\frac{1}{2})}\otimes H_1)^{\uparrow}G_1$, $b_8(\Phi_1^{(\frac{1}{2})}\otimes H_1)^{\uparrow}G_8$, $d_1(\Phi_1^{(\frac{3}{2})}\otimes H_2)^{\uparrow}G_1$, etc. is defined with appropriate Clebsch–Gordan (CG) coefficients while keeping in mind the symmetrization of the component wavefunction. The spin and color wavefunctions of sea are specified by $H_{0,1,2}$ and $G_{1,8,10}$. The spin-0 (1, 2) sea refers to the scalar (vector, tensor) sea. The coefficients (a_0, a_8, a_{10}, b_1, b_8, b_{10}, c_8, d_8) that appear in Eqs. (2) and (3) are the statistical parameters that contain the contribution of scalar, vector, and tensor sea. For octet baryonic wavefunctions, the parameters a_0, a_8, a_{10} give the contribution of the scalar sea, i.e. spin-0. Similarly, the parameters b_1, b_8, b_{10}, c_8 give the vector sea (spin-1) contribution and d_8 signifies the tensor sea (spin-2) contribution. These statistical parameters play an essential role in computing the various properties (spin distributions, masses, semileptonic decays) of baryons. Detailed information on the aforementioned wavefunctions can be found in Refs. [35,36].

3. Charge radii and quadrupole moment

The electromagnetic form factors of hadrons are used to understand their internal electric and magnetic structures. They describe the geometrical shape and spatial distributions of electric charge and current within the baryons and thus are intimately related to their intrinsic structure. Most of our experimental knowledge on electromagnetic structure comes from the elastic and inelastic scattering experiments (eN $\rightarrow e'\Delta$, $\gamma N \rightarrow \Delta$ transition) facilitated at various laboratories like Jefferson Lab, MIT-Bates, ELSA, MAMI, etc. [37,38]. It has been proposed that the $\Delta(1232)$ resonance, which is the lowest-lying excited state of the nucleon N(939), explains the charge distribution of nucleons in the ground state through the quadrupole deformation [39–41]. The N$\rightarrow$ Δ excitation (in short, $\gamma N\Delta$) is allowed the magnetic dipole (M1), electric quadrupole (E2), and charge (or Coulomb) quadrupole (C2) transition [42,43] modes due to the parity invariance and angular momentum conservation as shown in Fig. 1. The excitation

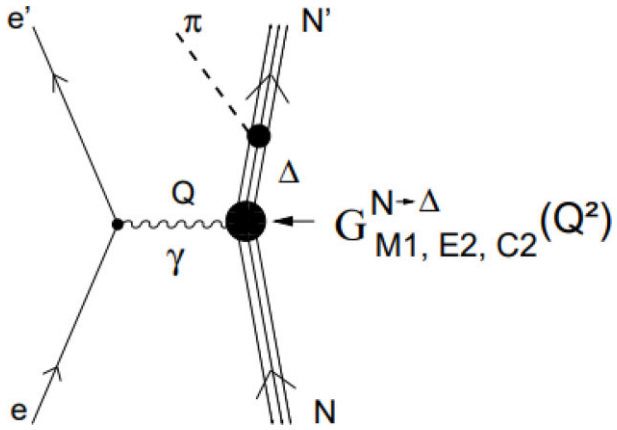

Fig. 1. The excitation of Δ-resonance is shown with inelastic electron–neutron scattering (e N→ $e'\Delta$), which is characterized by different electromagnetic transition form factors.

involves three transition form factors denoted as $G_{M1}^{N\to\Delta}(Q^2)$, $G_{E2}^{N\to\Delta}(Q^2)$, and $G_{C2}^{N\to\Delta}(Q^2)$. The measurement of nuclear deformation, rotation, and collective structure is dependent on electric quadrupole (E2) matrix elements that include quadrupole moments. The nonzero value of the E2 and C2 multipoles specifies that the distribution of charge within the nucleon deviates from spherical symmetry, but shows a dependency on angular orientation $\rho(r) = \rho(r, \theta, \Phi)$ [44,45]. For spherically symmetric charge distribution, the value of the E2 and C2 transition amplitudes would be zero. Many experiments have observed that at low momentum transfer, the magnetic dipole (M1) amplitude dominates in N (939)→ Δ(1232) excitation due to the flip of spin and isospin of a single quark. The measured ratio of the electric quadrupole to the magnetic dipole amplitude is $\frac{E2}{M1} = -0.025 \pm 0.005$ and the ratio of charge quadrupole to the magnetic dipole amplitude, i.e. $\frac{C2}{M1}$, has also been determined [17,46,47]. The nucleonic vertex function can be expressed in terms of Dirac and Pauli form factors $F_1(Q^2)$ and $F_2(Q^2)$ as:

$$\Gamma^{\mu} = F_1(Q^2)\gamma^{\mu} + \kappa F_2\left(Q^2\left(i\frac{\sigma^{\mu\nu}q_{\nu}}{2m}\right)\right) \tag{6}$$

Here, κ represent the anomalous part of the magnetic moment, γ^{μ} are Dirac matrices, and $\sigma^{\mu\nu} = i(\gamma_{\mu}\gamma_{\nu} - \gamma_{\nu}\gamma_{\mu})/2$. Further, the Sach form factors $G_E(Q^2)$ (electric) and $G_M(Q^2)$ (magnetic) can be related as [48]:

$$G_E = F_1 - \tau\kappa F_2 \tag{7}$$

$$G_M = F_1 + \kappa F_2 \tag{8}$$

where $\tau = (\frac{Q}{2m})^2$. The Fourier transform of the elastic form factors yields the radial variation of the charge ρ'(r) and current j′(r) densities. The charge density operator ρ' is expressed in its multipole expansion form up to the limit of q^2 as follows:

$$\rho'(q) = e - \frac{q^2}{6}r_B^2 - \frac{q^2}{6}Q_B + \ldots \tag{9}$$

Here q^2 represents the four-momentum transfer of the virtual photon. The initial two terms originate from the spherically symmetric monopole component, whereas the third term is derived from the quadrupole part of the charge density ρ'. These terms collectively describe the total charge (e), spatial extension (r_B^2), and shape (Q_B) of the system. The mean square charge

radii r_B^2 under spatial rotation is defined as:

$$\langle r_B^2 \rangle = \int d^3 r \rho'(r) r^2 \tag{10}$$

The deformity in the shape of baryons can be determined from the intrinsic quadrupole moment [49,50]:

$$Q_0' = \int d^3 r \rho'(r)(3z^2 - r^2) \tag{11}$$

If the charge density is predominantly distributed along the symmetry axis of the particle (in the z-direction), the term related to $3z^2$ governs, which will give a positive value of Q_0', resulting in a prolate shape. Conversely, if the charge density is concentrated in the equatorial plane perpendicular to z, the term associated with r^2 becomes more dominating, leading to a negative value of Q_0', and the particle exhibits an oblate shape. In order to determine the quadrupole moment of a baryon, a general QCD unitary operator and QCD eigenstates $|B\rangle$ are defined explicitly in terms of gluons and quarks. The quadrupole moment operator in terms of spin–flavor space can be expressed as [51,52]:

$$\widehat{Q}_B = B \sum_{i \neq j}^{3} e_i (3\sigma_{iz}\sigma_{jz} - \sigma_i.\sigma_j) + C \sum_{i \neq j \neq k}^{3} e_i (3\sigma_{jz}\sigma_{kz} - \sigma_j.\sigma_k) \tag{12}$$

Here, σ_{iz} represents the z-component of the Pauli spin matrix σ_i and e_i is the charge of the i^{th} quark where $i = (\text{u,d,s})$. The expansion of the quadrupole moment operator of octet and decuplet baryons [27] is expressed as:

$$\widehat{Q}_{1/2} = 3B \sum_{i \neq j} e_i \sigma_{iz} \sigma_{jz} + 3C \sum_{i \neq j \neq k} e_i \sigma_{jz} \sigma_{kz} + (-3B + 3C) \sum_i e_i \sigma_{iz} + 3B \sum_i e_i \tag{13}$$

$$\widehat{Q}_{3/2} = 3B \sum_{i \neq j} e_i \sigma_{iz} \sigma_{jz} + 3C \sum_{i \neq j \neq k} e_i \sigma_{jz} \sigma_{kz} + (-5B + 5C) \sum_i e_i \sigma_{iz} + (3B - 6C) \sum_i e_i \tag{14}$$

Further, the charge radii operator [24] can be presented as:

$$\widehat{r}_B^2 = A \sum_i e_i.1 + B \sum_{i \neq j} e_i \sigma_i \sigma_j + C \sum_{i \neq j \neq k} e_i \sigma_j \sigma_k \tag{15}$$

In the case of octet and decuplet baryons, the above expression of charge radii can be written as:

$$\widehat{r}_{1/2}^2 = (A - 3B) \sum_i e_i + 3(B - C) \sum_i e_i \sigma_{iz} \tag{16}$$

$$\widehat{r}_{3/2}^2 = (A - 3B + 6C) \sum_i e_i + 5(B - C) \sum_i e_i \sigma_{iz} \tag{17}$$

Here $\widehat{r}_{1/2}^2$ and $\widehat{r}_{3/2}^2$ represent the charge radii operator for spin-$\frac{1}{2}$ and spin-$\frac{3}{2}$ particles, respectively. The parameters A, B, and C are introduced in the operator's expansion, parametrizing the contribution of orbital and color space [29,30].

Using the operator formalism, the quadrupole moment and charge radii of octet and decuplet baryons are calculated. The matrix element of the operator corresponding to the spin–flavor

wavefunction is evaluated. For example, the charge radii of Σ^{*+} are illustrated as:

$$\left\langle \Phi_{3/2}^{(\uparrow)} | \widehat{O'} | \Phi_{3/2}^{(\uparrow)} \right\rangle = \frac{1}{N^2}\Big[{a_0}^2 \left\langle \Phi_1{}^{(\frac{3}{2}\uparrow)} | \widehat{O'} | \Phi_1{}^{(\frac{3}{2}\uparrow)} \right\rangle + {b_1}^2 \left\langle \Phi_1{}^{(\frac{3}{2}\uparrow)} | \widehat{O'} | \Phi_1{}^{(\frac{3}{2}\uparrow)} \right\rangle + b_8^2 \left\langle \Phi_8{}^{(\frac{1}{2}\uparrow)} | \widehat{O'} | \Phi_8{}^{(\frac{1}{2}\uparrow)} \right\rangle + {d_1}^2 \left\langle \Phi_1{}^{(\frac{3}{2}\uparrow)} | \widehat{O'} | \Phi_1{}^{(\frac{3}{2}\uparrow)} \right\rangle + {d_8}^2 \left\langle \Phi_8{}^{(\frac{1}{2}\uparrow)} | \widehat{O'} | \Phi_8{}^{(\frac{1}{2}\uparrow)} \right\rangle \Big] \tag{18}$$

Here, $\widehat{O'}$ represents the charge radii operator of the decuplet baryon mentioned in Eq. (17). After applying the operator, we get the expression in terms of the statistical coefficients (a_0, a_8, a_{10}, b_1, b_8, b_{10}, c_8, d_8) and the parameters A, B, and C:

$$\frac{1}{N^2}\Big[{a_0}^2(0.999A + 1.998B + 0.999C) + {b_1}^2(-0.9637A + 7.0022B - 9.8934C) + {b_8}^2(0.2101A + 4.036B - 3.4060C) + {d_1}^2(0.2A + 0.4B + 0.2C) + {d_8}^2(0.5333A - 1.1B + 2.7C)\Big] \tag{19}$$

Similar expressions are obtained for strange baryons in the SU(3) symmetry limit. The statistical coefficients are associated with the probability of each Fock state in flavor, spin, and color space individually. To determine the set of probabilities, a statistical method in conjugation with the detailed balance principle is used, discussed in the next section. The parameters A, B, and C were calculated in our previous article [53] using available experimental data for charge radii and quadrupole moment. We know that flavor SU(3) symmetry is an approximate symmetry; the different masses of up(u), down(d), and strange(s) quarks break SU(3) symmetry. To investigate the symmetry-breaking effect in valence, a mass-dependent parameter "r" is introduced in the operators. Upon applying the operators, the resulting eigenvalues are attained in the form of statistical coefficients and the breaking parameter "r." The obtained expressions for charge radii and quadrupole moment are tabulated in Tables 1 and 2, respectively.

4. Principle of detailed balance and statistical model

The detailed balance principle, put forward by Zhang et al. [54], posits that each physical hadron state can be expanded as an ensemble of quark–gluon Fock states. Each Fock state involves an infinite number of $q\bar{q}$ pairs mediated by gluons, which is expressed as:

$$|h\rangle = \sum_{i,j,k,l} C_{i,j,k,l} |\{q^3\}, \{i, j, k, l\}\rangle \tag{20}$$

Here $\{q^3\}$ is the constituent quarks of baryons, i, j, and l represent the number of quark–antiquark pairs, i.e. $u\bar{u}$, $d\bar{d}$, $s\bar{s}$ pairs, respectively, and k is the number of gluons. Basically, the quarks and gluons present in the Fock states are the intrinsic partons which are multiconnected nonperturbatively to the valence quarks [55]. It is important to mention that a confined gluon within the sea can be categorized into transverse electric (TE) mode with $J^{PC} = 1^{+-}$ and the transverse magnetic (TM) modes with $J^{PC} = 1^{--}$. To keep the parity of the system positive, Fock states with a single gluon are considered to be consisting of a TE mode. Similarly, Fock states with $q\bar{q}$ pairs are required to be in a p-wave state to maintain the positive parity of the system. The probability of finding the baryon in a quark–gluon Fock state $|\{q^3)\}, \{i, j, k, l\}\rangle$ is expressed as:

$$\rho_{i,j,k,l} = |C_{i,j,k,l}|^2 \tag{21}$$

where $\rho_{i,j,k,l}$ satisfy the normalization condition $\sum_{i,j,k,l} \rho_{i,j,k,l} = 1$.

Table 1. Certain expressions derived upon applying charge radii operators to $J^P = \frac{1}{2}^+$ octet and $J^P = \frac{3}{2}^+$ decuplet baryon wavefunctions.

Charge radii	Related expressions
$r^2_{\Sigma^{*+}}$	$a_0^2\,(0.7216 - 0.1804r) + b_1^2\,(3.8221 - 0.7780r) + b_8^2\,(1.7223 - 0.1643r) + d_1^2\,(0.1444 - 0.0361r) - d_8^2\,(0.7684 - 0.1921r)$
$r^2_{\Sigma^{*-}}$	$a_0^2\,(-0.3612 - 0.1806r) + b_1^2\,(-1.9111 - 0.7780r) + b_8^2\,(-0.8611 - 0.1643r) + d_1^2\,(-0.0722 - 0.0361r) + d_8^2\,(0.3842 + 0.1921r)$
$r^2_{\Sigma^{*0}}$	$a_0^2\,(0.1806 - 0.1806r) + b_1^2\,(0.2939 - 0.4714r) + b_8^2\,(0.4790 - 0.4790r) + d_1^2\,(0.0361 - 0.0361r) - d_8^2\,(0.2094 - 0.2094r)$
$r^2_{\Xi^{*-}}$	$a_0^2\,(-0.1806 - 0.3612r) + b_1^2\,(-0.2293 - 0.8136r) + b_8^2\,(-0.1643 - 0.8611r) + d_1^2\,(-0.1083 - 0.2167r) + d_8^2\,(0.1921 + 0.3842r)$
$r^2_{\Xi^{*0}}$	$a_0^2\,(0.3612 - 0.3612r) + b_1^2\,(1.685 - 2.0404r) + b_8^2\,(0.4256 - 0.9581r) + d_1^2\,(0.0722 - 0.0722r) - d_8^2\,(0.3842 - 0.3842r)$
$r^2_{\Omega^-}$	$a_0^2\,(-0.5418r) + b_1^2\,(-1.2204r) + b_8^2\,(-0.7128 - 0.2007r) + d_1^2\,(0.1503r) - d_8^2\,(-0.0846 + 0.6124r)$
$r^2_{\Sigma^+}$	$a_0{}^2\,(0.7851 + 0.0699r) + a_8{}^2\,(1.1369 + 0.2125r) + a_{10}{}^2\,(0.2527 - 0.0631r) + b_1{}^2\,(0.3136 - 0.1671r) + b_8{}^2\,(0.1598 - 0.2055r) + b_{10}{}^2\,(0.4911 - 0.1227r) + c_8{}^2\,(1.1691 - 0.2479r) + d_8{}^2\,(-0.4819 + 0.0938r)$
$r^2_{\Sigma^-}$	$a_0{}^2\,(-0.3925 + 0.0699r) + a_8{}^2\,(-0.5684 + 0.2125r) + a_{10}{}^2\,(-0.1263 - 0.0631r) + b_1{}^2\,(-0.1568 - 0.1671r) + b_8{}^2\,(-0.0799 - 0.2055r) + b_{10}{}^2\,(-0.2455 - 0.1227r) + c_8{}^2\,(-0.5845 - 0.2479r) + d_8{}^2\,(0.2409 + 0.0938r)$
$r^2_{\Sigma^0}$	$a_0{}^2\,(0.0534 - 0.1466r) + a_8{}^2(0.4411 - 0.5486r) + a_{10}{}^2\,(0.06319 - 0.1963r) + b_1{}^2\,(0.10757 - 0.08199r) + b_8{}^2\,(0.28425 - 0.30705r) + b_{10}{}^2\,(0.09298 - 0.04861r) + c_8{}^2\,(0.31448 - 0.2738r) + d_8{}^2\,(-0.0627 + 0.1093r)$
$r^2_{\Xi^-}$	$a_0{}^2\,(0.0699 - 0.3925r) + a_8{}^2\,(0.2125 - 0.5684r) + a_{10}{}^2\,(-0.0631 - 0.1263r) + b_1{}^2\,(-0.1671 - 0.1568r) + b_8{}^2\,(-0.2055 - 0.0799r) + b_{10}{}^2\,(-0.1227 - 0.2455r) + c_8{}^2\,(-0.2479 - 0.5845r) + d_8{}^2\,(0.0938 + 0.2030r)$
$r^2_{\Xi^0}$	$a_0{}^2\,(-0.1398 - 0.3925r) + a_8{}^2\,(-0.4251 - 0.5684r) + a_{10}{}^2\,(0.1263 - 0.1263r) + b_1{}^2\,(0.3343 - 0.1568r) + b_8{}^2\,(0.4111 - 0.0799r) + b_{10}{}^2\,(0.2455 - 0.2455r) + c_8{}^2\,(0.4958 - 0.5845r) + d_8{}^2\,(-0.1877 + 0.2030r)$
$r^2_{\Lambda^0}$	$a_0{}^2\,(0.05340 - 0.1466r) + a_8{}^2\,(0.4411 - 0.54868r) + a_{10}{}^2\,(0.06319 - 0.19631r) + b_1{}^2\,(0.10757 - 0.08199r) + b_8{}^2\,(0.2842 - 0.30705r) + b_{10}{}^2\,(0.09298 - 0.0486r) + c_8{}^2\,(0.3144 - 0.2738r) + d_8{}^2\,(-0.0627 + 0.1093r)$

This principle considers that any two neighboring quark–gluon Fock states should be in equilibrium with each other [56]. It means the probability of finding the baryon in any Fock state should remain constant over time and it is expressed as:

$$\rho_{i,j,k,l}|\{q^3\},\{i,j,k,l\}\rangle \rightleftharpoons \rho_{i',j',k',l'}|\{q^3\},\{i',j',k',l'\}\rangle$$

The transition probability of different Fock states in flavor space is calculated with the help of different subprocesses like $g \rightleftharpoons q\bar{q}$, $g \rightleftharpoons gg$, and $q \rightleftharpoons qg$. By taking the strange quark into consideration, the whole scenario is modified due to its large mass. To have transition processes like $g \rightleftharpoons s\bar{s}$, the gluons must have some free energy which should be greater than the mass of the strange quark, i.e. $\varepsilon_g > 2M_s$. The emergence of $s\bar{s}$ pairs from gluons is limited by a suppression factor which is formulated as $k(1 - C_l)^{n-1}$ [57], where n represents the total number of partons present in the Fock state. The factor arises from the distribution of free energy of gluons and

Table 2. Certain expressions derived upon applying quadrupole moment operators to $J^P = \frac{1}{2}^+$ octet and $J^P = \frac{3}{2}^+$ decuplet baryon wavefunctions.

Quadrupole moment	Related expressions
$Q_{\Sigma^{*+}}$	$a_0^2\,(-0.2586 + 0.06466r) + b_1^2\,(-0.4980 + 0.1096r) + b_8^2\,(-0.48117 + 0.09802r) + d_1^2\,(0.0485 + 0.0364r) - d_8^2\,(0.3898 - 0.04893r)$
$Q_{\Sigma^{*-}}$	$a_0^2\,(0.1293 + 0.0646r) + b_1^2\,(0.2490 + 0.1096r) + b_8^2\,(0.2405 + 0.0980r) + d_1^2\,(-0.0242 + 0.0364r) - d_8^2\,(-0.1949 - 0.074r)$
$Q_{\Sigma^{*0}}$	$a_0^2\,(-0.0646 + 0.0646r) + b_1^2\,(0.01582 - 0.0549r) + b_8^2\,(-0.0018 + 0.0358r) + d_1^2\,(0.0137 - 0.05284r) - d_8^2\,(-0.0212 + 0.02941r)$
$Q_{\Xi^{*-}}$	$a_0^2\,(0.06466 + 0.1293r) + b_1^2\,(0.1096 + 0.24902r) + b_8^2\,(0.0980 + 0.24059r) + d_1^2\,(0.0364 - 0.0242r) - d_8^2\,(0.074 - 0.19493r)$
$Q_{\Xi^{*0}}$	$a_0^2\,(-0.1293 + 0.1293r) + b_1^2\,(-0.2193 + 0.2490r) + b_8^2\,(-0.1960 + 0.24059r) + d_1^2\,(-0.1762 + 0.0792r) - d_8^2\,(0.0978 - 0.19493r)$
Q_{Ω^-}	$a_0^2\,(0.194r) + b_1^2\,(0.37113r) + b_8^2\,(0.35728r) + d_1^2\,(-0.13826r) - d_8^2\,(-0.2976r)$
Q_{Σ^+}	$a_0{}^2\,(0.00206r) + a_8{}^2\,(0.0107 + 0.0011r) + a_{10}{}^2\,(-0.00827 - 0.00206r) + b_1{}^2\,(0.1489 + 0.04320r) + b_8{}^2\,(0.22007 + 0.06114r) + b_{10}{}^2\,(-0.01608 + 0.00402r) + c_8{}^2\,(-0.3434 + 0.10647r) + d_8{}^2\,(-0.0223 + 0.0418r)$
Q_{Σ^-}	$a_0{}^2\,(0.00206r) + a_8{}^2\,(-0.00537 + 0.0011r) + a_{10}{}^2\,(0.00413 + 0.00206r) + b_1{}^2\,(-0.07446 + 0.04320r) + b_8{}^2\,(-0.14651 + 0.07684r) + b_{10}{}^2\,(0.00804 + 0.00402r) + c_8{}^2\,(0.1717 + 0.10647r) + d_8{}^2\,(0.0111 + 0.04188r)$
Q_{Σ^0}	$a_0{}^2\,(-0.01904 + 0.0240r) + a_8{}^2\,(-0.03312 + 0.03491r) + a_{10}{}^2\,(-0.03249 + 0.03145r) + b_1{}^2\,(-0.02099 + 0.00311r) + b_8{}^2\,(-0.03966 + 0.00666r) + c_8{}^2\,(0.09844 + 0.10230r) + d_8{}^2\,(-0.09654 + 0.10009r)$
Q_{Ξ^-}	$a_0{}^2\,(0.00206r) + a_8{}^2\,(0.00117 - 0.0053r) + a_{10}{}^2\,(0.0020 + 0.00413r) + b_1{}^2\,(0.0432 - 0.07446r) + b_8{}^2\,(0.07885 - 0.14249r) + b_{10}{}^2\,(0.00402 + 0.00804r) + c_8{}^2\,(0.1064 + 0.1717r) + d_8{}^2\,(0.04188 + 0.0111r)$
Q_{Ξ^0}	$a_0{}^2\,(-0.00413) + a_8{}^2\,(-0.0023 - 0.00537r) + a_{10}{}^2\,(-0.0041 + 0.00413r) + b_1{}^2\,(-0.0864 - 0.0744r) + b_8{}^2\,(-0.1517 - 0.14844r) + b_{10}{}^2\,(-0.0080 + 0.0080r) + c_8{}^2\,(-0.2129 + 0.1717r) + d_8{}^2\,(-0.0837 + 0.0111r)$
Q_{Λ^0}	$a_0{}^2\,(-0.01904 + 0.02402r) + a_8{}^2\,(-0.03312 + 0.03491r) + a_{10}{}^2\,(-0.03249 + 0.03145r) + b_1{}^2\,(-0.02099 + 0.00311r) + b_8{}^2\,(-0.03966 + 0.00666r) + c_8{}^2\,(0.09844 + 0.10230r) + d_8{}^2\,(-0.09654 + 0.10009r)$

the total energy of partons present in the baryon. For all cases, the value of $C_{l-1} = \frac{2M_s}{M_B - 2(l-1)M_s}$, where M_B is the mass of the baryon. It is important to note that the value of constraint $(1 - C_l)^{n-1}$ clearly indicates the difference between the double strange baryon and single strange baryon in accommodating $s\bar{s}$ pairs [58]. The increase in the number of $\bar{s}s$ pairs within doubly strange baryons leads to a decrease in the value of $(1 - C_l)^{n-1}$ and affects the overall probability of Fock states. The Fock states without strange quark content cover 86% of the total Fock states while the involvement of $s\bar{s}$ reduces this value to 80% [59]. The interesting part of taking the strange quark is that the separation and integration for the processes $g \rightleftharpoons s\bar{s}$ experience breaking in SU(3) symmetry within the sea. Detailed calculation of the probabilities including the strange $q\bar{q}$ condensates is given in Refs. [55,58,60].

Furthermore, the statistical decomposition of the baryons in different Fock states like $|u\bar{u}g\rangle$, $|d\bar{d}g\rangle$, $|s\bar{s}g\rangle$, $|u\bar{u}d\bar{d}\rangle$, and $|u\bar{u}d\bar{d}g\rangle$ is used to determine the probabilities in spin and color space

with their appropriate multiplicities. The multiplicities for all Fock states are computed as $\rho_{p,\,q}$ where the relative probability is associated with "Spin p" for the valence part and "Spin q" for sea components. Accordingly, the resultant spin should be $\frac{1}{2}$ ($\frac{3}{2}$) for octet (decuplet) baryons. In a similar manner, the color singlet states are obtained from the computed probabilities in color space. Detailed calculation of multiplicities is discussed in Refs. [55,58,59]. The sum of the total probabilities in spin, flavor, and color space will give the coefficients a_0, a_8, a_{10}, b_1, b_8, b_{10}, c_8, d_8 to the total wavefunction. The scalar, vector, and tensor sea contributions are expressed in terms of these coefficients. The statistical coefficients offer insights into how "sea quarks" contribute to diverse properties of baryons, including masses [61], semileptonic decays [62], charge radii [53], etc. The combination of the principle of detailed balance and statistical approach emerges as a reliable method for characterizing the various properties of baryons.

5. Numerical results and discussion

Probing the internal configuration of the ground and excited state baryons, the charge radii and electric quadrupole moment are the most interesting observables. To compute these properties, a suitable operator (discussed in Sect. 3) is applied to the baryonic wavefunction. Our key interest is to explore the significance of sea in the relative probabilities of Fock states containing both strange and nonstrange quark contents. The statistical coefficients represent the individual contribution of sea classified by their spin: scalar (spin-0), vector (spin-1), and tensor (spin-2) sea. In order to examine the contribution of scalar sea separately, we suppress the contributions of the vector sea and the tensor sea. The value of coefficients is assumed as $b_{1,\,8,\,10}$, c_8, $d_8 = 0$ for scalar sea, the coefficients $a_{0,\,8,\,10}$, $d_8 = 0$ for vector sea, and for tensor sea the coefficients are taken as $a_{0,\,8,\,10}$, $b_{1,\,8,\,10}$, $c_8 = 0$ for octet baryons. A similar analysis is applied to check the contribution of each individual sea for decuplet baryons. Due to the large mass difference of strange (s) and nonstrange quarks (u,d), we also studied the SU(3) symmetry and breaking effect on charge radii and quadrupole moments. To analyze the breaking of SU(3) symmetry within valence, a parameter "r" directly incorporates the strange quark mass into the relevant operator. The parameter "r" is defined as $r = \frac{\mu_s}{\mu_d}$ [35] where μ_s and μ_d are the magnetic moments of the strange and down quark, respectively. The dependence of m_s and $m_{u/d}$ is directly included in the parameter "r" with certain constants. The active involvement of the strange sea is taken into account through a suppression factor $(1 - C_l)^{n-1}$. This factor affects the probabilities of Fock states and consequently modifies the statistical coefficients. The statistical approaches include various models, i.e. Models C, P, and D, that enable us to explore the influence of sea dynamics on the several static properties of baryons [55]. Model C is the basic model that contains various quark–gluon Fock states and assumes the equal probability of each Fock state. Model D is a modified picture of Model C. The model suppresses the contribution of Fock states associated with higher multiplicities, introduced by Singh and Upadhyay [55]. Sea with greater multiplicity in color and spin space has less probability of survival due to higher interactions. We compute the charge radii and quadrupole moment using Model D, presented in Tables 3 and 4. Apart from this, it is important to mention that using an appropriate fitting procedure, the best-fit value of "r" is obtained as $r = 0.850$. Also, the parameters mentioned in operators, i.e. A, B, and C, are used as input which was calculated previously in Ref. [53] by the χ^2 minimization method.

5.1. *Charge radii*

The charge radii hold interest in providing detailed information on the spatial distribution of charge inside the baryons. It is influenced by various factors such as masses of the constituent quarks and their specific flavor composition. Using the statistical framework, the numerical data on electric charge radii for octet $J^P = \frac{1}{2}^+$ and decuplet $J^P = \frac{3}{2}^+$ particles are presented in Table 3. The statistical coefficients provide the significant contribution of the strange and nonstrange $q\bar{q}$ condensates.

5.1.1. $J^P = \frac{3}{2}^+$ *baryons.* For decuplet particles (Σ^{*-}, Σ^{*+}, Ξ^{*-}, Ω^-), the scalar sea acts as a major contributor from the total sea. One reason for this is possibly the higher multiplicities of valence spin states when interacting with the spin of sea quarks (i.e., spin-0, -1, and -2). The chances of having spin-$\frac{3}{2}$ are greater when paired with spin-0 (scalar sea) in contrast to spin-1, -2 (vector, tensor sea). Although the vector and tensor sea contribution is less, it cannot be neglected. In the SU(3) symmetry limit, the contribution of pure scalar sea to the charge radii is more than 90% whereas the vector and tensor sea contributed nearly 2%–8%. For neutral particles, i.e. Ξ^{*0}, Σ^{*0}, only the vector sea contributes while the impact of the scalar and tensor sea is zero. This occurs because of the zero contribution of the valence quark wavefunction corresponding to the scalar sea (a_0) and tensor sea (d_1, d_8) terms. If the strange sea is assumed then the following points are observed to the forefront:

(1) For Σ^{*-}(dds), Ξ^{*-}(dss), Ω^-(sss) baryons, a decrease in charge radii value is observed in Table 3. This may be possible due to the larger mass of the strange quark that limits the free energy of gluons, which affects the emission of virtual gluons. As a result, the Fock states with large numbers of $s\bar{s}$ pairs are assumed to be less probable. It also indicates that the charge radii of baryons are directly influenced by the probabilities associated with accommodating $s\bar{s}$ pairs. On the other side, the value of charge radii is increased for Σ^{*+}(uus), Σ^{*0}(uds), Ξ^{*0}(uss) baryons. In addition to the quark-mass dependence, the electric charge of quarks is also a crucial factor that influences the charge radii of baryons. Due to the high charge of the up(u) quark, possibly the strength of electromagnetic interaction dominates for $u\bar{u}$ as compared to $d\bar{d}$, $s\bar{s}$ condensates.

(2) For neutral particles, i.e. Σ^{*0}, Ξ^{*0}, the scalar sea becomes an active contributor, as the effect of the vector and tensor sea is much less and it can be neglected. The presence of the mass correction parameter "r" ensured that the valence quark contribution across the scalar sea (a_0) cannot be zero. In the SU(3) symmetry limit, the decuplet baryon charge radii can be illustrated as:

$$r^2_{\Sigma^{*+}} = r^2_{\Sigma^{*-}} = r^2_{\Xi^{*-}} = r^2_{\Omega^-}$$

The symmetry breaking modifies the pattern considerably, and we get

$$r^2_{\Sigma^{*+}} > r^2_{\Sigma^{*-}} > r^2_{\Xi^{*-}} > r^2_{\Omega^-}$$

The charge radii value deviates 4%–10% when compared with the SU(3) symmetry results. We observed a considerable change in both the magnitude and sign of charge radii of neutral strange baryons (Σ^{*0}, Ξ^{*0}) after incorporating the strange sea. The changes in the charge radii of Σ^{*0}, Ξ^{*0} closely match the lattice QCD predictions [25,26], as shown in Table 5.

5.1.2. $J^P = \frac{1}{2}^+$ *baryons.* In the case of octet particles, the sea is found to be dynamic for vector plus scalar sea within SU(3) symmetry. The tensor sea contribution is negligible for all the baryons because of the quark spin-flip processes. The contribution of the scalar sea is about 50%–80%, whereas the vector sea contributed about 15%–50% to the charge radii of $J^P = \frac{1}{2}^+$ particles. The neutral particles (Σ^0, Λ^0) have zero valence quark contribution. Further, when the strange sea is considered, the contribution of individual sea (scalar, vector, and tensor) exhibits similar dominancy to the SU(3) symmetry. The interesting point is observed that the charge radii value is decreased for doubly strange particles (Ξ^0, Ξ^-) and increased for singly strange baryons (Σ^+, Σ^-). It may be possible because when doubly strange baryons accommodate large numbers of $s\bar{s}$ pairs in the sea, the value of the suppression factor $(1 - C_l)^{n-1}$ decreases, and it automatically decreases the probability of that particular Fock state as discussed in the preceding section. The chances of the interaction of sea having $s\bar{s}$ pairs with heavier strange baryons are less as compared to lighter strange baryons. Moreover, within the SU(3) symmetry limit we get the following pattern for the octet charge radii:

$$r^2_{\Sigma^+} > r^2_{\Xi^-} > r^2_{\Xi^0} > r^2_{\Sigma^-}$$

However, the results changed after considering the breaking of SU(3) symmetry:

$$r^2_{\Sigma^+} > r^2_{\Sigma^-} > r^2_{\Xi^-} > r^2_{\Xi^0}$$

The relevance of the sea can be understood by the suppression of higher multiplicities of the different quark–gluon Fock states. If the sea is entirely excluded in the statistical model, the charge radii show a variation of more than 50% from the computed values. Various phenomenological models [24–28,30] predicted the different values of charge radii of octet and decuplet baryons. Table 5 shows the comparison of our computed results with various theoretical models.

5.2. *Quadrupole moment*

The quadrupole moment is an important structural property that characterizes the charge distribution within the baryons and gives insights into the deformities in the shape of the baryon. This deformation is related to the angular momentum and spin of the valence quarks. The statistical model is sensitive to the probabilities related with color, spin, and flavor space. By using this approach, we computed the numerical results of the quadrupole moment of $J^P = \frac{1}{2}^+, \frac{3}{2}^+$ baryons, which are presented in Table 4.

5.2.1. $J^P = \frac{3}{2}^+$*baryons.* For decuplet particles (Σ^{*-}, Σ^{*+}, Ξ^{*-}, Ω^-), the scalar sea acts as a major contributor from the total sea. For neutral particles, i.e. Ξ^{*0}, Σ^{*0}, only the tensor sea contributed while the effect of the scalar and vector sea is negligible. The vector and tensor sea contributed 4%–10% whereas the scalar sea contribution to the quadrupole moment is about 88%. It shows that the possibility of having valence spin-$(\frac{3}{2})^+$ is higher with the scalar sea (spin-0) as compared to the vector and tensor sea. On incorporating the effect of the strange sea, a few points need to be addressed:

(1) The value of the quadrupole moment is decreased for negatively charged particles, i.e. Σ^{*-}(dds), Ξ^{*-}(dss), Ω^-(sss), and increased for Σ^{*+}(uus), Σ^{*0}(uds), Ξ^{*0}(uss) baryons. The variation in the value of the quadrupole moment is influenced by the splitting and recombination between gluons and $s\bar{s}$ pairs undergoing the process $g \rightleftharpoons s\bar{s}$. Instead of this, the breaking parameter "r," associated with the strange baryons, contributes to the

Table 3. Numerical outcomes of charge radii measured in units of [fm^2] taking the symmetry-breaking parameter value $r = 0.850$.

		Statistical model								
Baryons	Charge radii	SU(3) symmetry with (scalar + vector + tensor) sea	Scalar sea	Vector sea	Tensor sea	SU(3) symmetry breaking with (valence + sea)	Scalar sea	Vector sea	Tensor sea	Without sea
Σ^{*+}	$0.71084 - 0.17665r$	0.5347	0.5127	0.0170	0.0048	0.5611	0.5381	0.0177	0.0050	4.675
Σ^{*-}	$-0.35576 - 0.17682r$	−0.5325	−0.5127	−0.0149	−0.0048	−0.5061	−0.4872	−0.0143	−0.0045	−3.788
Σ^{*0}	$0.17585 - 0.17737r$	−0.0015	0.0	−0.0015	0.0	0.0249	0.0256	−0.0008	0.0	−0.177
Ξ^{*-}	$-0.17733 - 0.35895r$	−0.5362	−0.5082	−0.0123	−0.0157	−0.4827	−0.4576	−0.0108	−0.0141	−2.359
Ξ^{*0}	$0.36149 - 0.36578r$	−0.0042	0.0	−0.0042	0.0	0.0503	0.0505	−0.0007	0.0	−0.887
Ω^-	$0.00007 - 0.52970r$	−0.5325	−0.5318	−0.0007	0.0027	−0.4530	−0.4524	−0.0006	0.0023	−1.198
Σ^+	$0.63812 - 0.062899r$	0.5752	0.4527	0.1227	−0.0003	0.5846	0.4470	0.1379	−0.0003	3.396
Σ^-	$-0.33284 - 0.033445r$	−0.3601	−0.2001	−0.1664	0.0003	−0.3612	−0.2069	−0.1546	0.0003	−2.343
Σ^0	$0.13594 - 0.18124r$	0.0	–	–	–	−0.0182	−0.0373	0.0190	0.0	−0.1995
Ξ^-	$-0.03814 - 0.35289r$	−0.3910	−0.1953	−0.1960	0.0	−0.3383	−0.1595	−0.1791	0.0003	−2.381
Ξ^0	$-0.02696 - 0.34976r$	−0.3767	−0.4189	0.0421	0.0	−0.3245	−0.3733	0.0489	0.0	−1.090
Λ^0	$0.11881 - 0.170227r$	0.0	–	–	–	−0.0260	−0.0361	0.0101	0.0	−0.1994

Table 4. Numerical outcomes of quadrupole moments measured in units of [fm^2] taking the symmetry-breaking parameter value $r = 0.850$.

		Statistical model								
Baryons	Quadrupole moment	SU(3) symmetry with (scalar + vector + tensor) sea	Scalar sea	Vector sea	Tensor sea	SU(3) symmetry breaking with (valence + sea)	Scalar sea	Vector sea	Tensor sea	Without sea
Σ^{*+}	$-0.24520 + 0.06353r$	-0.1817	-0.1836	-0.0022	0.0041	-0.1911	-0.1927	-0.0023	0.0039	-0.539
Σ^{*-}	$0.12260 + 0.06351r$	0.1861	0.1836	0.0020	0.0004	0.1766	0.1744	0.0019	0.0001	0.634
Σ^{*0}	$-0.06087 + 0.05902r$	-0.0018	0.0	-0.0003	-0.0015	-0.0106	-0.0091	-0.0002	-0.0012	-0.036
Ξ^{*-}	$0.06370 + 0.12293r$	0.1866	0.1819	0.0042	0.0004	0.1682	0.1638	0.0037	0.0006	0.634
Ξ^{*0}	$-0.13256 + 0.12805r$	-0.0045	0.0	0.003	-0.0048	-0.0236	-0.0181	0.0	-0.0005	-0.119
Ω^{-}	$0.18816r$	0.1881	0.1904	0.0002	-0.0024	0.1600	0.1619	0.0	-0.0021	0.502
Σ^{+}	$0.02333 + 0.035296r$	0.0667	0.0012	0.0653	0.0	0.0533	0.0010	0.0523	0.0	0.257
Σ^{-}	$-0.01805 + 0.03079r$	0.0020	0.0011	0.0007	0.0	0.0081	0.0009	0.0071	0.0	0.246
Σ^{0}	$-0.03602 + 0.02883r$	0.0	–	–	–	-0.0114	0.0006	-0.0121	0.0	-0.1018
Ξ^{-}	$0.03262 - 0.00346r$	0.0362	0.0011	0.0349	0.0001	0.0296	0.0011	0.0284	0.0	0.252
Ξ^{0}	$-0.03152 - 0.01404r$	-0.0422	-0.003	-0.038	0.0	-0.0434	-0.0032	-0.0400	-0.0001	-0.586
Λ^{0}	$-0.034183 + 0.031026r$	0.0	–	–	–	-0.0077	0.0007	-0.0084	-0.1018	0.116

change in the quadrupole moment value. From the results, we can suggest that the charge distribution inside the baryons is symmetric or in a compact manner for the negatively charged particles (Σ^{*-}, Ξ^{*-}, Ω^{-}) as compared to other baryons.

(2) For neutral (Σ^{*0}, Ξ^{*0}) particles, the dominancy of the pure scalar sea can be easily observed from Table 4. This implies that the major contribution came from the spin-0, indicating the interaction of gluons. The impact of the vector and tensor sea can be neglected. The magnitude of the quadrupole moments of decuplet baryons can be presented as follows.
With SU(3) symmetry:

$$Q_{\Sigma^{*+}} = Q_{\Sigma^{*-}} = Q_{\Xi^{*-}} = Q_{\Omega^{-}}$$

With SU(3) symmetry breaking:

$$Q_{\Sigma^{*-}} > Q_{\Xi^{*-}} > Q_{\Omega^{-}} > Q_{\Sigma^{*0}} > Q_{\Xi^{*0}} > Q_{\Sigma^{*+}}$$

In the statistical model, we predicted an oblate shape for Σ^{*+}, Σ^{*0}, Ξ^{*0} baryons and a prolate shape for Σ^{*-}, Ξ^{*-}, Ω^{-}. On comparison with SU(3) symmetry results, the quadrupole moment value deviates up to 14% for Σ^{*-}, Σ^{*+}, Ξ^{*-}, Ω^{-} baryons and the deviation is maximum for neutral baryons (Σ^{*0}, Ξ^{*0}) at more than 80%. This signifies the impact of strange sea quarks with strange baryons. We compared our predicted results with different theoretical models [27–30], as shown in Table 5. Our computed results are in good agreement with Refs. [27,28] with error up to 20%.

5.2.2. $J^P = \frac{1}{2}^+$ *baryons.* The emission of virtual gluons dominates the sea, suggesting that the vector sea coefficients b_1, b_8, c_8 are likely to be more dominating. From Table 4, we can observe the vector sea dominancy in relation to the quadrupole moment value. The contribution of the vector sea is more than 95%. For each particle, the scalar and tensor sea contribution is nearly negligible. Also, neglecting the tensor sea is based on the fact that the tensor sea contribution comes from the spin-$\frac{3}{2}$ valence part and the probability for the core part to have spin-$\frac{3}{2}$ is very much less. Neutral baryons, i.e. Σ^0, Λ^0, exhibit quadrupole moment values of zero. The magnitude of the quadrupole moment within the SU(3) symmetry limit can be expressed as:

$$Q_{\Sigma^{+}} > Q_{\Xi^{0}} > Q_{\Xi^{-}} > Q_{\Sigma^{-}}$$

Also, we have

$$Q_{\Sigma^{0}} = Q_{\Lambda^{0}}$$

where the valence part gives zero contribution to the quadrupole moment value. On accounting for the strange sea, the contribution of individual sea (scalar, vector, and tensor) exhibits similarity with the nonstrange sea. Due to the symmetry-breaking effect, we observed that the quadrupole moment decreases for Ξ^{-}(dss) and increases for Σ^{-}(dds). This is because higher masses of quarks have lesser chances than the lighter quarks due to the limited energy of gluons. On the contrary, we note an increase in the quadrupole moment for the Ξ^{0}(uss) and a decrease for the Σ^{+}(uus) baryon. In lieu of, the mass correction parameter "r" and sea quarks producing a non-vanishing value for the neutral baryons (Σ^0, Λ^0). Further, the magnitude of the quadrupole moment with symmetry-breaking effect can be represented as:

$$Q_{\Sigma^{+}} > Q_{\Xi^{0}} > Q_{\Xi^{-}} > Q_{\Sigma^{0}} > Q_{\Sigma^{-}} > Q_{\Lambda^{0}}$$

Table 5. Comparison of our computed results for symmetry breaking of charge radii and quadrupole moment with available experimental data and other theoretical models.

Baryons	Quadrupole moment	χCQM [27,28]	GPM [29,30]	Skyrme [63,64]	Charge radii	Expt. value	Lattice [25,26]	χCQM [27]	GPM [29,30]
Σ^{*+}	−0.1911	−0.1808	−0.153	−0.42	0.5611	–	0.399	0.978	1.086
Σ^{*-}	0.1766	0.1942	0.115	0.52	−0.5061	–	−0.360	1.038	0.845
Σ^{*0}	−0.0106	0.0067	−0.0019	0.05	0.0249	–	0.020	−0.030	0.127
Ξ^{*-}	0.1682	0.1954	0.071	0.35	−0.4827	–	−0.330	1.043	0.692
Ξ^{*0}	−0.0236	0.0079	−0.029	−0.07	0.0503	–	0.043	−0.035	0.244
Ω^{-}	0.1600	0.1966	0.040	0.24	−0.4530	–	–	0.355	0.553
Σ^{+}	0.0533	−0.032	–	–	0.5846	–	0.749	0.767	0.928
Σ^{-}	0.0081	0.009	–	–	−0.3612	0.61	0.657	0.664	0.672
Σ^{0}	−0.0114	−0.012	–	–	−0.0182	–	–	0.052	0.128
Ξ^{-}	0.0296	0.009	–	–	0.3383	–	0.502	0.669	0.520
Ξ^{0}	−0.0434	−0.019	–	–	−0.3245	–	−0.082	−0.120	0.132
Λ^{0}	−0.0077	–	–	–	−0.0260	–	0.010	−0.063	0.050

On comparison with SU(3) symmetry results, the quadrupole moment value deviates up to 30% with the maximum deviation exceeding 50% for the Σ^- baryon. Using the statistical approach we predicted a prolate shape for the Σ^+, Σ^-, Ξ^- baryons and an oblate shape for the Σ^0, Ξ^0, Λ^0 neutral baryons. In order to exclude the sea completely in the statistical model, the quadrupole moment for both $J^P = \frac{1}{2}^+$ and $J^P = \frac{3}{2}^+$ baryons deviates more than 50% from the calculated value. From Table 5, it can be observed that our computed results in sign and magnitude are consistent with various phenomenological models [27,29,30]. Since no experimental information is available on the quadrupole moment, the accuracy of our results can be assessed by future experiments.

6. Conclusion

In our present work, the statistical approach is applied to calculate the electromagnetic properties, i.e. charge radii and quadrupole moment, of strange baryons. Baryons are assumed to have a virtual dynamic sea with strange and nonstrange $q\bar{q}$ condensates in addition to gluons. Our main focus of attention is to analyze the impact of strange and nonstrange partons on the aforementioned properties. The principle of detailed balance is used to determine the probabilities for quark–gluon Fock states in terms of statistical parameters (a_0, a_8, a_{10}, b_1, b_8, b_{10}, c_8, d_8). To appreciate the strange sea, a strangeness suppression factor $(1 - C_l)^{n-1}$ is discussed which modifies all the probabilities related to different Fock states. It also induces a breaking in SU(3) symmetry within the sea. To study the breaking effect on valence, the relevant operator involved the parameter "r," which is directly related to the mass of the strange quark. Our analysis concluded that, for $J^P = \frac{3}{2}^+$ particles, the scalar sea is the major contributor to both properties. In the case of $J^P = \frac{1}{2}^+$ particles, the charge radii are mainly influenced by the scalar plus vector sea, whereas the quadrupole moment is primarily dominated by the vector sea. The strange sea seems to contribute effectively, and gluons are responsible for the splitting and recombination of strange $q\bar{q}$ condensates. The statistical approach predicts an oblate shape for Σ^{*+}, Σ^{*0}, Ξ^{*0}, Σ^0, Ξ^0, Λ^0 baryons and a prolate shape for Σ^+, Σ^-, Ξ^-, Σ^{*-}, Ξ^{*-}, Ω^- baryons. The analysis of the quadrupole moment concludes that the strange sea quarks influence the overall structure of baryons without causing a change in their shape. We summarize that the strange sea caters for a more effective SU(3) analysis concerning both charge radii and quadrupole moment. It is

worthwhile to mention that our calculations are performed in a nonrelativistic frame with the energy scale of order 1 GeV^2.

Funding

Open Access funding: SCOAP[3]. The authors gratefully acknowledge the financial support by the Department of Science and Technology (SERB/F/9119/2020), New Delhi.

References

[1] C. Quintans, Few Body Syst. **63**, 72 (2022).
[2] G. Huang and R. Baldini Ferroli, [BESIII Collaboration], Natl. Sci. Rev. **8**, 11 (2021).
[3] J. Adam et al. [STAR Collaboration], Phys. Rev. D **99**, 051102 (2019).
[4] W. M. Alberico, S. M. Bilenky, and C. Maieron, Phys. Rep. **358**, 227 (2002).
[5] D. S. Armstrong and R. D. McKeown, Annu. Rev. Nucl. Part. Sci. **62**, 337 (2012).
[6] J. A. Jaros and M. E. Peskin, Int. J. Mod. Phys. A **15**, 521 (2000).
[7] M. Goncharov et al., Phys. Rev. D **64**, 112006 (2001).
[8] D. T. Spayde et al. [SAMPLE Collaboration], Phys. Lett. B **583**, 79 (2004).
[9] K. A. Aniol et al. [HAPPEX Collaboration], Phys. Rev. C **69**, 065501 (2004).
[10] K. A. Aniol et al. [HAPPEX Collaboration], Eur. Phys. J. A **31**, 597 (2007).
[11] Z. Ahmed et al. [HAPPEX Collaboration], Phys. Rev. Lett. **108**, 102001 (2012).
[12] F. E. Maas et al. [PVA4 Collaboration], Phys. Rev. Lett. **94**, 152001 (2005).
[13] G. Barruca et al. [PANDA Collaboration], Eur. Phys. J. A **57**, 184 (2021).
[14] G. Barruca et al. [PANDA Collaboration], Eur. Phys. J. A **55**, 42 (2019).
[15] H. B. Li et al. [BESIII Collaboration], PoS (Flavor physics and CP Violation), (2011). [arXiv:2204.08943] [hep-ex][Search inSPIRE].
[16] K. Aoki et al. [J-PARC Facility], [arXiv:2110.04462v1] [nucl-ex], (2021). [Search inSPIRE].
[17] R. L. Workman et al. [Particle Data Group], Prog. Theor. Exp. Phys. **2022**, 083C01 (2022) .
[18] R. K. Sahoo, A. R. Panda, and A. Nath, Phys. Rev. D **52**, 4099 (1995).
[19] G. Ramalho and K. Tsushima, Phys. Rev. D **87**, 093011 (2013).
[20] T. Liu and B. Ma, Phys. Rev. D **92**, 096003 (2015).
[21] Y. Liu, M. Huang, and D. Wang, Eur. Phys. J. C **60**, 593 (2009).
[22] K. Azizi, Eur. Phys. J. C **61**, 311 (2009).
[23] R. F. Lebed and D. R. Martin, Phys. Rev. D **70**, 016008 (2004).
[24] A. J. Buchmann and R. F. Lebed, Phys. Rev. D **67**, 016002 (2003).
[25] C. Alexandrou, G. Koutsou, J. W. Negele, Y. Proestos, and A. Tsapalis, Phys. Rev. D **83**, 014501 (2011).
[26] S. Boinepalli, D. B. Leinweber, P. J. Moran, A. G. Williams, J. M. Zanotti, and J. B. Zhang, Phys. Rev. D **80**, 054505 (2009).
[27] N. Sharma and H. Dahiya, Pramana **80**, 237 (2013).
[28] H. Dahiya and N. Sharma, Light Cone: Relativistic Hadronic and Particle Physics, 056 (2010).
[29] A. J. Buchmann and E. M. Henley, Phys. Rev. C **63**, 015202 (2001).
[30] A. J. Buchmann and E. M. Henley, Phys. Rev. D **65**, 073017 (2002).
[31] A. Kaur and A. Upadhyay, Eur. Phys. J. A **52**, 332 (2016).
[32] M. Batra and A. Upadhyay, Int. J. Mod. Phys. A **28**, 1350062 (2013).
[33] A. Kaur and A. Upadhyay, Eur. Phys. J. A **52**, 105 (2016).
[34] M. Batra and A. Upadhyay, Nucl. Phys. A **889**, 18 (2012).
[35] X. Song and V. Gupta, Phys. Rev. D. **49**, 2211 (1994).
[36] A. Kaur, PhD thesis, Thapar University, http://hdl.handle.net/10266/6081 (2018).
[37] C. F. Perdrisat, V. Punjabi, and M. Vanderhaeghen, Prog. Part. Nucl. Phys. **59**, 694 (2007).
[38] V. Punjabi, C. F. Perdrisat, M. K. Jones, E. J. Brash, and C. E. Carlson, Eur. Phys. J. A **51**, 79 (2015).
[39] L. Tiator, D. Drechsel, S. S. Kamalov, and S. N. Yang, Eur. Phys. J. A **17**, 357 (2003).
[40] G. Blanpied et al. (The LEGS Collaboration), Phys. Rev. Lett. **79**, 4337 (1997).
[41] G. Blanpied et al. Phys. Rev. C **64**, 025203 (2001).
[42] A. J. Buchmann, Phys. Rev. Lett. **93**, 212301 (2004).

[43] R. Beck et al., Phys. Rev. Lett., **78**, 606 (1997).
[44] A. M. Bernstein and C. N. Papanicolas, AIP Conf. Proc. **904**, 1 (2007).
[45] V. Pascalutsa, M. Vanderhaeghen, and S. N. Yang, Phys. Rep. **437**, 125 (2007).
[46] P. Grabmayr and A. J. Buchmann, Phys. Rev. Lett. **86**, 2237 (2001).
[47] A. J. Buchmann, Phys. Rev. Lett. **93**, 212301 (2004).
[48] M. K. Jones et al. [The Jefferson Lab Hall A Collaboration], Phys. Rev. Lett. **84**, 1398 (2000).
[49] M. Eisenberg and W. Greiner, Nuclear models. Amsterdam: North-Holland; 1970.
[50] P. Brix and Z. Naturforsch, Teil A, **41A**, 3 (1986).
[51] G. Dillon and G. Morpurgo, Phys. Lett. B **448**, 107 (1999).
[52] A. J. Buchmann and E. M. Henly, Phys. Rev. D **65**, 073017 (2002).
[53] P. Bhall, M. Batra, and A. Upadhyay, Prog. Theor. Exp. Phys. **2023**, 093B03 (2023).
[54] Y. J. Zhang, W. Z. Deng, and B. Q. Ma, Phys. Rev. D **65**, 114005 (2002).
[55] J. P. Singh and A. Upadhyay, J. Phys. G **30**, 881 (2004).
[56] Y. J. Zhang, B. Q. Ma, and L. Yang, Int. J. Mod. Phys. A **18**, 14651468 (2003).
[57] Y. J. Zhang, B. Zhang, and B. Q. Ma, Phys. Rev. D **65**, 114005 (2002).
[58] A. Kaur and A. Upadhyay, Eur. Phys. J. A **52**, 105 (2016).
[59] M. Batra and A. Upadhyay, Nucl. Phys. A **922**, 126 (2014).
[60] M. Batra and A. Upadhyay, Int. J. Mod. Phys. A **28**, 1350062 (2013).
[61] A. Kaur and A. Upadhyay, Eur. Phys. J. A **52**, 332 (2016).
[62] A. Upadhyay and M. Batra, Eur. Phys. J. A **49**, 160 (2013).
[63] B. Schwesinger and H. Weigel, Nucl. Phys. A **540**, 461 (1992).
[64] J. Kroll and B. Schwesinger, Phys. Lett. B **334**, 287 (1994).

Funded by SCOAP³.